Influence of Solvent Quality and Thermal Fluctuations on Polymer-Mediated Depletion Interactions

Avik P. Chatterjee and Kenneth S. Schweizer*

Departments of Materials Science & Engineering and Chemistry, and Materials Research Laboratory, University of Illinois, 1304 West Green Street, Urbana, Illinois 61801

Received September 16, 1998; Revised Manuscript Received December 1, 1998

ABSTRACT: Analytic integral equation theory for treating athermal mixtures of hard spheres and polymers is extended to study thermal interaction and solvent quality effects in suspensions of infinitely dilute spherical particles in dilute and semidilute polymer solutions. Our approach applies to all sphere/polymer size ratios, and polymer−polymer segmental attractive interactions are included using both liquid state and Flory−Huggins theory. The effect of such thermal interactions on the polymer-induced depletion potential between hard spheres is studied with emphasis on the sphere−sphere second virial coefficient and the free energy of particle insertion. Strong enhancement of the purely entropic attractive depletion interaction is found in the proximity of the polymer−solvent critical demixing point. The magnitude of this effect and the distance from the Θ temperature where it becomes important are sensitive to system-specific factors.

I. Introduction

In recent work, we have developed an analytic polymer reference interaction site model (PRISM) integral equation-based theory[1] for describing polymer-induced interactions between hard spherical particles of arbitrary size. In this earlier "athermal" study,[1] all the pairwise interaction potentials had been assumed to be hard core repulsions, corresponding to the problem of polymer-induced depletion attractions of a purely entropic packing origin.[2−4] Our microscopic approach accounts for the fact that polymer molecules are connected chains of elementary monomer or segmental units and does not approximate them by effectively spherical macromolecular entities. For such model athermal systems, the theory based on the Percus−Yevick (PY) closure predicts a significantly weaker entropic depletion attraction between large colloidal spheres[1] than found by theories which represent the polymer as a phantom ideal coil[5] or as a hard impenetrable sphere[2,6,7] (in relation to its interactions with particles) of size given by the radius of gyration R_g. The relation between our athermal system integral equation predictions and those of prior phenomenological,[2,5] scaling,[8] and field theoretic[9] approaches, connections with computer simulations[10,11] and experiments,[12,13] and possible deficiencies of the PY closure in the large colloidal sphere limit has been presented in great detail elsewhere.[1] The athermal theory has been generalized to include nonadditivity in the hard core diameters,[14] a feature relevant to understanding polymer-mediated interactions between coated colloidal particles. The present paper takes the first step toward explicitly including thermal interactions and examines the consequences of decreasing solvent quality.

A treatment which includes thermal polymer−polymer segmental interactions addresses a weakness of our earlier work,[1] which modeled chains under "Θ" conditions by assuming ideal chain statistics ($R_g \sim \sqrt{N}$) while simultaneously asserting that the only *inter*chain interactions were of a hard core excluded volume type. It is known that, under athermal (good solvent) conditions, individual chains are swollen relative to their ideal dimensions at dilute and semidilute concentrations; the Flory ideality condition obtains only at higher concentrations and in the melt.[15] Inclusion of thermal interaction effects in the theory is important for properly modeling both single chain and intermolecular polymer correlations and thermodynamic properties such as the polymer osmotic pressure, under Θ-like conditions, and also for understanding more completely the corresponding polymer-induced depletion potential. Since the Θ temperature is, for long chains, very close to the polymer−solvent critical demixing temperature,[15] the possibility exists for long-wavelength critical polymer density fluctuations to couple to and strongly modify the polymer-induced potential of mean force between particles relative to that calculated for the purely hard core athermal situation. This generalization of our approach may also be relevant to understanding charged systems, such as suspensions of polyelectrolytes with charged spheres.[6]

To place the new thermal results in proper context, our theory for the athermal problem is briefly summarized in section II. Section III discusses the generalization to include thermal polymer−polymer interactions; analytic results and model calculations illustrating the consequences of thermal effects on the polymer density screening length, sphere−sphere second virial coefficient, and free energy of insertion are presented. The paper concludes in section IV with a discussion. Some results relevant to including thermal contributions to the polymer−particle and particle−particle interactions are given in the Appendix.

II. PRISM Theory for Athermal Systems

As in previous work,[1] R_g and R denote the coil radius of gyration and the polymer segment-colloid particle distance of closest approach ($R \equiv d_{pc}$), respectively. Though we investigate the entire range of size ratios between the spherical particles and polymer coils, we

* To whom correspondence should be addressed at the Department of Materials Science & Engineering.

10.1021/ma981473h CCC: $18.00
Published on Web 01/22/1999

shall for brevity refer at times to the spherical solute as the "colloidal" species. The polymer and colloid site number densities are ρ_p and ρ_c, respectively; σ is the effective statistical segment length of the model chains. The subscripts "p" and "c" denote "polymer" and "colloid", respectively. The polymer site number density will often be written in a dimensionless form in terms of the reduced density variable $z \equiv \rho_p\sigma^3$. The symbols ρ^*_p and z^* denote the values of ρ_p and z at the crossover from dilute to semidilute polymer concentrations[15]; ρ^*_p is defined as $\rho^*_p \equiv 3N/4\pi R_g^{(0)\,3}$, where $R_g^{(0)}$ is the coil radius of gyration under dilute condition. N is the number of interaction sites per chain, proportional to the degree of polymerization. The distance of closest approach between spherical particle centers will be represented by d_{cc}. In this work we consider exclusively the case of "additive" diameters, i.e., $d_{cc} \equiv 2R$.

Polymer−colloid suspensions are in reality three-component systems containing solvent molecules. Our theory does not include the solvent particles explicitly and treats instead an effective two-component system in which only the polymer molecules and colloid particles are represented. The effect of solvent condition may be accounted for at the single chain level by the effect on the statistical segment length or chain dimensions, and the terms polymer concentration/density are used interchangeably, as the polymer molecules are the only component present at finite concentration in our present work. This treatment is analogous to our previous investigation of demixing in polymer solutions in terms of an effective one-component model in which only the polymer molecules were represented explicitly.[16] The liquid−vapor transition in this effective one-component system was correlated with liquid−liquid-phase separation into polymer-rich and polymer-poor phases.

Within the PRISM approach, which generalizes the small molecule RISM theory of Chandler and Andersen to macromolecules,[17] the Ornstein−Zernike-like matrix equations for a two-component system in Fourier space are[18]

$$\hat{h}_{MM'}(k) = \hat{\omega}_M(k)[\hat{C}_{MM'}(k)\hat{\omega}_{M'}(k) + \sum_{M''}\hat{C}_{MM''}(k)\rho_{M''}\hat{h}_{M''M'}(k)] \quad (1)$$

where ρ_M and $\hat{\omega}_M(k)$ are, respectively, the site number density and the intramolecular structure factors for species M, $h_{MM'}(r) \equiv g_{MM'}(r) - 1$, $g_{MM'}(r)$ is the intermolecular site−site pair correlation function between species M and M', and $C_{MM'}(r)$ is the corresponding direct correlation function. The single chain structure factor, $\hat{\omega}_p(k)$, is assumed to be given by the following Lorentzian form:

$$\hat{\omega}_p(k) = \frac{1}{1/N + k^2\sigma^2/12} \quad (2)$$

Here N and σ are, respectively, the number of sites per chain and the effective statistical segment length. The coil radius of gyration, R_g is, $\sqrt{N/6}\sigma$. The Lorentzian expression closely approximates the Debye form factor for flexible chains[15] over the entire range of wavevector k, and permits development of an analytic theory. Use of eq 2 with analytic PRISM theory has been shown to provide a consistent description of thermodynamic properties of homogeneous polymer solutions at dilute and semidilute concentrations, for *both* Θ *and* good solvent conditions.[19] The Θ solvent case is realized by choosing σ in eq 2 to be independent of N and ρ_p. Choice of the appropriate dependence of σ on N and ρ_p to recover chain swelling under dilute condition and the scaling theory prediction for the dependence of R_g on ρ_p in the semidilute regime allows a consistent description of the good solvent situation.[19]

In the present paper, the single chain conformations are assumed to be ideal at *all* temperatures. This simplification, which is equivalent to treating the effective segment length σ as a constant independent of temperature, N, and polymer concentration, permits a clear-cut evaluation of the influence of thermal polymer−solvent interactions *alone* and will be accurate close to the Θ or critical temperature. A complete theory would calculate the single chain conformations self-consistently as functions of the polymer density and solvent quality/temperature. Though such more complicated approaches have been developed within the PRISM framework,[20,21] we refrain from this elaboration in the present work.

We employ the analytic thread polymer model[18] which corresponds to taking the limit $d_{pp} \to 0$, where d_{pp} is the hard core diameter for individual thread polymer segments or sites. The polymer−polymer site−site direct correlation function $C_{pp}(r)$ is represented as a Dirac delta function in position space, in the spirit of a Percus−Yevick (PY) site−site closure approximation:[18]

$$C_{pp}(r) = C_{pp}\delta(\mathbf{r}); \quad \hat{C}_{pp}(k) = C_{pp} \quad (3)$$

The excluded volume constraint between chain segments is enforced in a pointwise manner by requiring that the interchain segmental pair correlation vanish as $r \to 0$, i.e., that $g_{pp}(r \to 0) = 0$. In the limit that the colloidal species is infinitely dilute ($\rho_c = 0$), the three coupled PRISM equations (see eq 1) decouple into an independent equation for $\hat{h}_{pp}(k)$ and a pair of coupled equations for $\hat{h}_{pc}(k)$ and $\hat{h}_{cc}(k)$ which can be solved once $\hat{h}_{pp}(k)$ has been determined. Use of eqs 1−3 together with the pointwise core condition for the polymer−polymer pair correlation function leads to the following expression[18] for $g_{pp}(r)$ when $\rho_c = 0$:

$$g_{pp}(r) = 1 + \frac{3\sigma}{\pi z r}[e^{-r/\xi_\rho} - e^{-r/\xi_c}] \quad (4)$$

$$\frac{\sigma}{\xi_\rho} = \frac{\sigma}{\xi_c} + \frac{\pi z}{3}; \quad \xi_c^{\,2} = \frac{N\sigma^2}{12} \quad (5)$$

$$\rho_p C_{pp} = \frac{1}{N} - \frac{1}{12}\left(\frac{\sigma}{\xi_\rho}\right)^2 \quad (6)$$

The polymer−polymer collective structure factor is $\hat{S}_{pp}(k) \equiv \hat{\omega}_p(k) + \rho_p\hat{h}_{pp}(k)$ and is given by

$$\hat{S}_{pp}(k) = \frac{12}{k^2\sigma^2 + \sigma^2/\xi_\rho^{\,2}} \quad (7)$$

The polymer osmotic pressure under athermal conditions is

$$\beta\sigma^3 P(z) = \int_0^z dz_1 \hat{S}_{pp}^{-1}(0; z_1) = \frac{z}{N} + \frac{\pi}{36}\left(\frac{\sigma}{\xi_c}\right)z^2 + \frac{\pi^2 z^3}{324} \quad (8)$$

where $z \equiv \rho_p\sigma^3$ Equation 5 for the polymer density dependence of the screening length ξ_ρ, together with the

use of a ρ_p- and N-dependent effective segment length σ for good solvent conditions, have been shown to be accurate at dilute and semidilute concentrations.[19]

An analytic theory of polymer solutions within an effective one-component model has been developed[19] based on eqs 1−3 to account approximately for the finite chain diameter d_{pp}. Inclusion of finite chain thickness effects leads to a different expression for ξ_ρ than that in eq 5, but which reduces to eq 5 at dilute and semidilute concentrations for long chains. Use of this Gaussian "string model" leads to a more rapid, non-power law growth in the athermal pressure at high polymer concentrations.[19] The applicability of eq 5 is therefore limited to dilute and semidilute concentrations, i.e., to $\rho_p < \rho^{**}_p$. The present work focuses on polymer densities below the semidilute/concentrated solution crossover ρ^{**}_p (typically ≈25−30% polymer by volume). We next summarize previously obtained solutions[1] to the athermal PRISM integral equations for $h_{pc}(r)$ and $h_{cc}(r)$ in the limit that the spheres are infinitely dilute.

Equations 1 and 4−7 determine the polymer−colloid correlation function $\hat{h}_{pc}(k)$ according to

$$\hat{h}_{pc}(k) = \hat{C}_{pc}(k)\hat{S}_{pp}(k) = \frac{12\hat{C}_{pc}(k)}{\sigma^2(k^2 + 1/\xi_\rho^{\,2})} \tag{9}$$

to be solved subject to the hard core exclusion condition that $h_{pc}(r) = -1$ for $r < R$. For athermal hard core systems and $r > R$, we employ the PY closure, which gives

$$C_{pc}(r) = C^{(1)}_{pc}(r) - \frac{\sigma^2}{12R}\left[1 + \frac{R}{\xi_\rho}\right]\delta(r - R)$$

$$C^{(1)}_{pc}(r) = \frac{-\sigma^2}{12\xi_\rho^{\,2}}, \quad r < R$$

$$= 0, \; r > R$$

$$h_{pc}(r) = -1, \quad r < R$$

$$= -\left(\frac{R}{r}\right)e^{-(r-R)/\xi_\rho}, \quad r > R \tag{10}$$

Equation 10 shows that the contact value for $g_{pc}(r)$, i.e., $g_{pc}(r = R)$, vanishes; thus $g_{pc}(r)$ is predicted to be *continuous* across $r = R$, although its slope is not. Integration of $C_{pc}(r)$ yields

$$\hat{C}_{pc}(k = 0) \equiv C_{pc} = -\frac{\pi R\sigma^2}{3}\left[\frac{1}{3}\left(\frac{R}{\xi_\rho}\right)^2 + \frac{R}{\xi_\rho} + 1\right] \tag{11}$$

The quantity $-k_BTC_{pc}$ is a measure of the effective repulsive interaction strength between polymer sites and a spherical particle.

The colloid−colloid correlations obey[1]

$$\hat{h}_{cc}(k) = \hat{C}_{cc}(k) + \frac{12\rho_p\hat{C}_{pc}^{\,2}(k)}{\sigma^2(k^2 + 1/\xi_\rho^{\,2})}$$

$$= \hat{C}_{cc}(k) + \hat{W}(k)$$

$$\hat{W}(k) = \rho_p\hat{C}_{cp}(k)\hat{S}_{pp}(k)\hat{C}_{pc}(k) \tag{12}$$

The inverse Fourier transform of $\hat{W}(k)$, denoted $W(r)$, is the polymer-mediated contribution to the colloid−colloid total correlation function. It contains contributions to all orders in the polymer density ρ_p, and has a range given by the screening length ξ_ρ of density fluctuations in the polymer solution. Equations 9, 10, and 12 yield:

$$W(r) = \frac{\pi z}{144}\left(\frac{R}{\sigma}\right)\left(\frac{R}{\xi_\rho}\right)^2\left[\left(2 - \frac{r}{R}\right)\left(8 - \frac{2r}{R} - \frac{r^2}{R^2} + \frac{24\xi_\rho}{R}\right) + 12\left(\frac{\xi_\rho}{R}\right)^2\left(4 - \frac{r}{R}\right)\right], \quad 0 < r < 2R$$

$$W(r) = \frac{\pi z}{3}\left(\frac{R}{r}\right)\left(\frac{R}{\sigma}\right)e^{-(r-2R)/\xi_\rho}, \quad r > 2R \tag{13}$$

The colloid−colloid correlations in r space thus become

$$h_{cc}(r) = C_{cc}(r) + W(r) \tag{14}$$

where $W(r)$ is a positive definite, monotonically decreasing function of r.

Determination of $h_{cc}(r)$ from eq 14 requires an additional closure relation. Use of the PY approximation for the athermal colloid−colloid problem leads to[1]

$$g_{cc}(r) = 0, \quad r < d_{cc}$$

$$g_{cc}(r) = 1 + W(r), \quad r > d_{cc} \tag{15}$$

where d_{cc} is the hard sphere diameter between colloidal particles. Note that the function $W(r)$ in eq 13 depends on the polymer-colloid distance of closest approach R, but is *independent* of d_{cc}. The value of $g_{cc}(r)$ at contact, $g_{cc}(r = 2R)$, is

$$g_{cc}\,(r = 2R) = 1 + \frac{\pi z}{6}\left(\frac{R}{\sigma}\right) \tag{16}$$

and is independent of the polymer screening length ξ_ρ. The polymer-induced effect on $g_{cc}(r)$ is *purely attractive* at *all* values of r and polymer density ρ_p; addition of polymer is predicted to *always* enhance colloid−colloid clustering at all separations for the athermal problem.

A general expression for the dimensionless free energy of sphere insertion into a polymer solution is given within the compressibility route to the thermodynamics by[1,22]

$$\beta\delta\mu_c = -\int_0^{\rho_p} d\rho'_p\hat{C}_{pc}(0; \rho'_p)$$

$$= \frac{1}{9}\left[\frac{R^3}{\xi_\rho^{\,3}} - \frac{R^3}{\xi_c^{\,3}}\right] + \frac{1}{2}\left[\frac{R^2}{\xi_\rho^{\,2}} - \frac{R^2}{\xi_c^{\,2}}\right] + \frac{R}{\xi_\rho} - \frac{R}{\xi_c} \tag{17}$$

where $\xi_c = R_g/\sqrt{2}$ is the correlation hole length scale, the polymer density ρ_p is integrated from zero to the desired value, and the athermal screening length is given by eq 5. The colloid−colloid second virial coefficient B_2^{cc} relative to the bare hard sphere value B_2^{HS} is[23]

$$\frac{B_2^{cc}}{B_2^{HS}} = -\frac{3\hat{h}_{cc}(k = 0; \rho_p)}{32\pi R^3}$$

$$= 1 - \frac{\pi z}{4}\left(\frac{\xi_\rho}{\sigma}\right)\left[1 + \frac{\xi_\rho}{2R}\right] \tag{18}$$

where the second line follows from eqs 13−15. Note that eqs 17 and 18 are *not* limited to the athermal situation, but within the Lorentzian approximation of eq 7, they

apply also to cases in which thermal interactions are treated at the level of a temperature-dependent polymer density screening length ξ_ρ. Under athermal conditions, eqs 5 and 18 predict that B_2^{cc} is positive (repulsive) for *all* values of the polymer concentration in the "colloid limit" ($R \gg R_g$) . In the "protein limit" ($R \ll R_g$), B_2^{cc} exhibits a negative (attractive) minimum near the semidilute crossover ρ^*_p, but at higher polymer densities becomes positive (repulsive) again.[1] Qualitative physical interpretation of these results, along with discussion of their expected accuracy, has been given in ref 1.

III. Inclusion of Polymer−Polymer Thermal Interactions

Effective (solvent-mediated) thermal interactions between polymer segments may be simply included by introducing a temperature-dependent screening length or mesh size ξ_ρ^{th} in the polymer−polymer structure factor $\hat{S}_{pp}(k)$ of eq 7. We shall explicitly consider the common "upper critical solution temperature" (UCST) phase behavior corresponding to low-temperature polymer−solvent phase separation.[15] However, when interpreted in the more general language of polymer screening length (as opposed to T) as a measure of phase stability, our results may be of qualitative value for polymer−solvent systems which undergo a heating-induced LCST phase separation.[24]

For analytic convenience, we employ an effective polymer−polymer segmental attractive interaction $v(r)$ of the Yukawa form

$$v(r) = -|\epsilon|(a/r)e^{-r/a} \tag{19}$$

specified by the range a and strength $\epsilon = -|\epsilon| < 0$. The effect of $v(r)$ on the correlation functions $g_{MM'}(r)$ and thermodynamics is incorporated by suitable modification of the closure approximation. Previous work has explored in detail predictions of alternative closure approximations for the polymer−solvent demixing transition.[16] For present purposes, we restrict ourselves to the linearized reference molecular Percus−Yevick/high-temperature approximation (RMPY/HTA),[25] which has proved quite successful in describing phase transitions in polymer solutions, blends, and diblock copolymer systems.[16,18,26,27] For the $d_{pp} \to 0$ thread limit, the RMPY/HTA closure approximation corresponds to the following equation for the temperature-dependent direct correlation function $C_{pp}(\mathbf{r})$:

$$C_{pp}(\mathbf{r}) = C_{pp}^{(0)}\delta(\mathbf{r}) - \beta v(r) g_{pp}^{(0)}(r) \tag{20}$$

where $C_{pp}^{(0)}$ and $g_{pp}^{(0)}(r)$ are the athermal values for the direct correlation strength parameter and interchain segmental pair correlation functions, respectively. Equation 20 specifying C_{pp} under thermal conditions may be viewed as a thermodynamic perturbation theory implemented at the level of the direct correlation function.

The spinodal boundary for the liquid−vapor transition in the effective one-component polymer solution model within the RMPY/HTA closure is[16]

$$\frac{t_s^{HTA}}{\Theta} = \frac{\pi z\delta + \dfrac{3}{\left(1 + \dfrac{\delta}{\xi_c} + \dfrac{\pi z\delta}{3}\right)} - \dfrac{3}{\left(1 + \dfrac{\delta}{\xi_c}\right)}}{3\left(\dfrac{\delta}{\xi_c} + \dfrac{\pi z\delta}{3}\right)^2} \tag{21}$$

where the spinodal temperature $t_s^{HTA} \equiv k_B T_s^{HTA}/|\epsilon|$ is in units of the effective polymer−polymer thermal interaction energy $|\epsilon|$, $\Theta \equiv 144\delta^4$ is the limiting long chain value of the Θ temperature at which the polymer−polymer second virial coefficient vanishes, and $\delta \equiv a/\sigma$ and is of order unity. Equation 21 shows that t_s^{HTA}/Θ is a function of the variables z/z^* and R_g/a *alone*. The N dependences of the critical density z_c^{HTA} and critical temperature t_c^{HTA} (where $t_c \equiv k_B T_c/|\epsilon|$) within this closure approximation have been investigated in earlier work, and show the following asymptotic behaviors in the long chain limit[16]

$$z_c^{HTA} \sim (\delta N)^{-1/3}, \quad 1 - t_c^{HTA}/\Theta \sim \delta^{2/3} N^{-1/3} \tag{22}$$

where z_c^{HTA}/z^* depends on a and R_g through the variable R_g/a *alone*. The above predictions for the asymptotic behaviors of z_c^{HTA} and t_c^{HTA}, and for the spinodal boundary, are to be contrasted with those of the widely used mean field Flory−Huggins theory,[28] which makes the following predictions for the spinodal curve and critical point parameters:

$$t_s/\Theta = \frac{N\phi(1-\phi)}{1 + (N-1)\phi}, \quad \phi_c^{FH} = \frac{1}{1+\sqrt{N}}, \quad 1 - t_c^{FH}/\Theta \approx 2/\sqrt{N} \tag{23}$$

Here, ϕ_c^{FH} and t_c^{FH} are the polymer volume fraction at the critical point and the dimensionless critical temperature, respectively. Note the different exponents for the N dependences of the critical polymer density or volume fraction predicted by the PRISM RMPY/HTA and Flory−Huggins theories. Experiments[29] and simulations[30] on phase-separating polymer solutions typically find an N dependence of the critical volume fraction of $N^{-0.38}$, which is intermediate between the $\sim 1/\sqrt{N}$ behavior predicted by Flory−Huggins theory and the asymptotic $\sim N^{-1/3}$ obtained from PRISM theory with the RMPY/HTA closure; our predictions in eq 22 based on the thread model are also consistent with results of numerical PRISM calculations performed on finite thickness semiflexible chains.[31]

Use of the linearized RMPY/HTA closure, together with the Lorentzian form assumed for $\hat{\omega}_p(k)$ in eq 2, shows that under thermal conditions the polymer−polymer partial structure factor $\hat{S}_{pp}(k)$ may still be approximated by a Lorentzian:

$$\hat{S}_{pp}(k) = \frac{12}{\sigma^2\left(k^2 + \left(\dfrac{1}{\xi_\rho^{ath}}\right)^2\left(1 - \dfrac{t_s}{t}\right)\right)} \tag{24}$$

This is valid so long as the athermal value for the density screening length ξ_ρ^{ath} is large compared to the thermal interaction range a, a condition *always* true for $\rho_p \ll \rho^{**}_p$ when $v(r)$ is a short-range dispersion-type attraction. The above result is not restricted to the RMPY/HTA closure alone but applies also to other implementations of thermal liquid-state theory[18] which express $\hat{C}_{pp}(k = 0)$ as a *linear* function of $\beta \equiv 1/k_B T$. Alternative theories for the spinodal boundary may also be employed to obtain the z and N dependence of t_s for

use in eq 24. Here we also consider the incompressible Flory−Huggins theory[28] for $t_s(N,z)$. Equations 9, 12, and 24 show that *all* of our previous results for the athermal problem may be generalized to the thermal case by introducing a temperature-dependent thermal screening length ξ_ρ^{th}

$$\xi_\rho^{ath} \rightarrow \xi_\rho^{th} \equiv \xi_\rho^{ath}/\sqrt{1 - t_s/t} \tag{25}$$

where the screening length under athermal conditions, ξ_ρ^{ath}, is given by eq 5. The temperature dependence is of a classic mean field form, which is expected to be valid in polymer solutions except very close to the critical point.[32] On the basis of the RMPY/HTA closure result for the spinodal boundary, the ratio ξ_ρ^{th}/R_g is seen from eqs 5, 21, and 25 to be a function of the three dimensionless variables R_g/a, z/z^*, and t/Θ.

Effects due to proximity in temperature to a polymer−solvent critical demixing point enter purely through the enhancement of ξ_ρ, and the colloid−colloid contact value $g_{cc}(d_{cc})$ (eq 16) is *not affected* by the polymer−polymer thermal interactions. Thus the *strength* of the attractive polymer-induced potential of mean force between spheres at contact is *not* affected, but the *range* of this interaction, given by ξ_ρ^{th}, can be greatly enhanced if the system is "near enough" a critical point that long-wavelength polymer density fluctuations become perceptible. This mechanism for strengthening the depletion attraction will be shown to have important consequences for B_2^{cc} which is sensitive to *both* the strength *and* range of the potential of mean force.

A. Thermal Effects on ξ_ρ. Equation 25 shows that thermal enhancement of ξ_ρ at a fixed temperature is maximal near the critical polymer density. Depending on the precise shape of the spinodal boundary $t_s(z)/\Theta$, nonmonotonic polymer density dependence of ξ_ρ^{th} at fixed t/Θ may be possible. For the RMPY/HTA theory of the polymer−solvent spinodal, we note the following: (i) the asympototic behaviors of eq 22, (ii) the fact that the scaled spinodal temperature t_s/Θ is a function of the variables $x \equiv z/z^*$ and a/R_g *alone*, and (iii) the fact that for densities higher than the critical density z_c and $R_g \gg a$, the RMPY/HTA spinodal boundary is well approximated by

$$\frac{t_s}{\Theta} \approx \frac{1}{1 + \dfrac{\pi\delta z}{3}} \tag{26}$$

where $\delta \equiv a/\sigma$. The spinodal temperature as a function of polymer concentration predicted by the Flory−Huggins theory was given in eq 23. Our discussion will focus primarily on the Θ temperature ($t = \Theta$); at temperatures between Θ and the athermal limit ($t \rightarrow \infty$), the screening length will show behaviors intermediate between those discussed here and the athermal result of eq 5. However, it is of considerable practical experimental interest to understand how much larger than unity the ratio t/Θ (or t/t_s) must be for effectively athermal solvent quality conditions to apply.

For the polymer situation where $R_g \gg a$, the following qualitative picture emerges for the dependence of ξ_ρ^{th} on z at $t \equiv \Theta$. For densities $z \leq z_c^{HTA} \sim N^{-1/3}$, ξ_ρ^{th} remains approximately constant at its athermal zero-density (dilute) value of $R_g/\sqrt{2}$; the influence of the thermal interactions is to prevent the decay seen in ξ_ρ^{ath} for $z > z^* \sim N^{-1/2}$. Because $z_c^{HTA} > z^*$, ξ_ρ^{th} does *not* exhibit a maximum as a function of z; the critical density is in the (weakly) semidilute regime, where ξ_ρ^{ath} is a decreasing function of z, and the thermal interactions at Θ are just strong enough to arrest that decay for $z \leq z_c^{HTA}$. For $z > z_c^{HTA}$, t_s decreases in accordance with eq 26, with a power law behavior $\xi_\rho^{th}/\sigma \sim z^{-3/2}$, which is to be contrasted with the $\sim 1/z$ dependence shown by ξ_ρ^{ath} at these densities. This stronger power law dependence found at $t = \Theta$ is due to the steady decrease in t_s/Θ; the thermal enhancement of ξ_ρ, which is at a maximum at z_c^{HTA}, is reduced at higher densities, until when $z \approx \sigma/a$, the thermal effect becomes negligible and ξ_ρ regains its athermal value, which at this density is $\xi_\rho \approx a$. These qualitative results are visible in the model calculations in Figure 1, which shows predictions for ξ_ρ^{th} at several temperatures. As t is lowered from infinity (athermal) toward Θ, note the emergence of a density regime over which ξ_ρ^{th} is effectively constant and $\approx \xi_c$; as $t \rightarrow \Theta$, this domain extends up to the critical density z_c^{HTA}, and the physical picture of the polymer solution as an ideal gas of mutually penetrable random coils is appropriate. It is very significant to note that this predicted behavior is in excellent agreement with recent experiments[33] which indicate that, at the Θ temperature, ξ_ρ^{th} is effectively independent of polymer concentration below ρ^*_p. At reduced polymer densities greater than z_c^{HTA}, Figure 1 shows the stronger decay of ξ_ρ^{th} relative to ξ_ρ^{ath} due to the decrease in t_s.

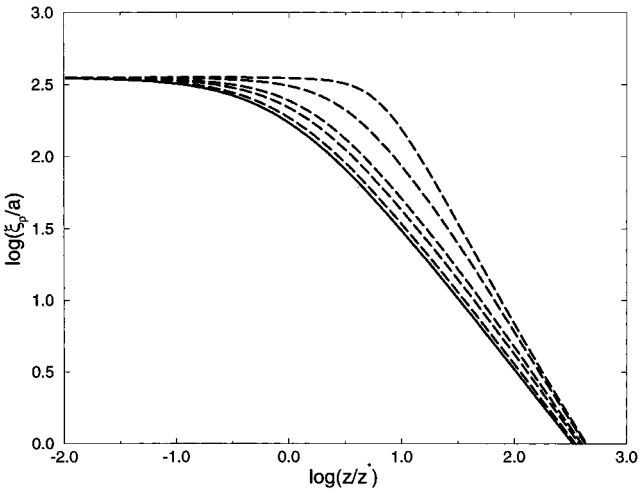

Figure 1. Logarithm of the dimensionless thermal density screening length calculated from the RMPY/HTA theory as a function of the logarithm of the reduced polymer density. In all cases, $R_g = 500a$, and the solid line represents the $t/\Theta \rightarrow \infty$ athermal result. The dashed lines correspond to $t/\Theta = 5$, 2, 1.5, 1.1, and 1.0 from bottom to top.

Equations 2, 5, and 7 show that equating the screening length ξ_ρ^{th} to its value ξ_c under $\rho_p = 0$ conditions is equivalent to replacing the polymer−polymer structure factor $\hat{S}_{pp}(k)$ by the single chain structure factor $\hat{\omega}_p(k)$ in the PRISM eq 1. Such a replacement corresponds to a physical situation in which the polymer solution behaves effectively as an ideal gas of interpenetrable coils, *but* where the coils *do* experience excluded volume interactions with respect to the spherical "solute" particles. These circumstances are similar to the unbalanced excluded volume assumptions underlying some prior treatments[2,5] of the depletion interaction which

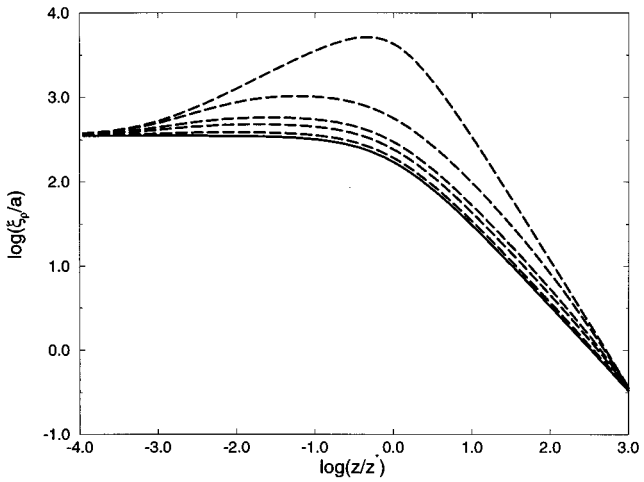

Figure 2. Same as Figure 1 but based on Flory−Huggins theory for ξ_ρ^{th}.

make use of the phantom-coil approximation to model the polymer−polymer interaction. Such an approximation may indeed be appropriate at (or near) $t = \Theta$ for polymer concentrations $z \leq z_c$. At higher polymer concentrations, the spinodal temperature steadily decreases below Θ, and the polymer−polymer excluded volume interaction causes the screening length ξ_ρ^{th} to decline with increasing z.

Qualitatively different behavior for ξ_ρ^{th} is predicted by use of the Flory−Huggins theory for t_s/Θ as a function of polymer density and N. To enable direct comparison, we choose the constant of proportionality between the reduced polymer density z and the volume fraction ϕ in the Flory−Huggins model such that in the long chain limit, the critical volume fraction ϕ_c equals the semidilute crossover concentration z^* in our model, which both behave as $\sim N^{-1/2}$. This mapping is implemented through the relation $\phi^{FH} = 2\pi z^{PRISM}/9\sqrt{6}$. The equality of ϕ_c with the semidilute crossover z^*, and the fact that in the Flory−Huggins model t_c^{FH}/Θ is closer to unity than for the RMPY/HTA theory of the spinodal, lead to stronger thermal effects on ξ_ρ in the former case. Thus, ξ_ρ^{th} *increases* with polymer density z at low densities (below $z_c^{FH} \approx z^*$), and, at $z = z_c^{FH}$, is larger than R_g in an N-dependent way, given approximately by $\xi_\rho^{th}(\phi = \phi_c, t = \Theta) \sim N^{3/4}$. For densities above z_c^{FH}, ξ_ρ^{th} drops as Θ/t_s becomes larger and regains the athermal zero-density value $\propto R_g$ at a density $z_1 > z_c^{FH}$ which scales such as $z_1 \sim N^{-1/3}$; the equality of the exponent in the N dependence of z_1 with that of the critical density z_c in the RMPY/HTA closure is purely accidental. At higher densities, use of the Flory−Huggins theory yields a ξ_ρ^{th} which again shows a stronger dependence on z than in the athermal case; as in the RMPY/HTA theory for the spinodal, we find that $\xi_\rho^{th} \sim z^{-3/2}$ for $z > z_1$. The important difference from the RMPY/HTA case is that, *in contrast to experiment*,[32,33] ξ_ρ^{th} at the Θ temperature is predicted to exceed R_g near the semidilute overlap concentration, and the thermal enhancement relative to ξ_ρ^{ath} is notably stronger. These differences carry over into the behaviors of B_2^{cc} and $\beta\delta\mu_c$, which we discuss in the next section.

Model calculations of ξ_ρ^{th} from eq 25 using the Flory−Huggins theory for t_s/Θ shown in Figure 2 display all the expected qualitative trends discussed above.

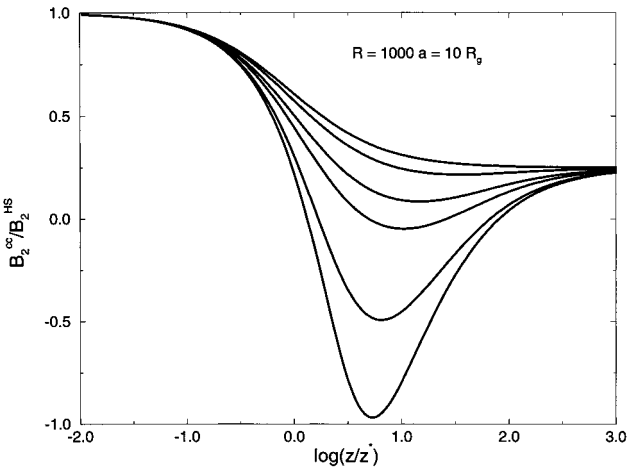

Figure 3. B_2^{cc}/B_2^{HS} as a function of $\log(z/z^*)$ under thermal conditions based on the RMPY/HTA closure in the $R \gg R_g$ colloid limit. In all cases, $R = 10^3 a$ and $R_g = 10^2 a$; the curves correspond to $t/\Theta = \infty$, 5, 2, 1.5, 1.1, and 1.0 from top to bottom.

B. Thermal Effects on B_2^{cc}. The sphere−sphere second virial coefficient B_2^{cc} follows from eq 18 with the thermal screening length ξ_ρ introduced in eq 25. To highlight the sensitivity of the predicted behavior to details of the thermal screening length, we consider both the Flory−Huggins and RMPY/HTA theories for the polymer concentration dependence of t_s/Θ.

Within the RMPY/HTA closure, eqs 5, 18, 21, and 25 show that B_2^{cc}/B_2^{HS} under thermal conditions is a function of the variables z/z^*, R/R_g, a/R_g, and t/Θ. The thermal enhancement of ξ_ρ leads at fixed z, R, and R_g to a stronger depletion effect and a more attractive (more negative) value of B_2^{cc}/B_2^{HS}. In the colloid limit ($R \gg R_g$), reducing the temperature from the athermal limit toward Θ leads to appearance of a minimum near z_c^{HTA} in the curve for B_2^{cc}/B_2^{HS} as a function of z; near enough to Θ, and if R/R_g is not too large, B_2^{cc} can become negative at this point. Including thermal interactions thus significantly and qualitatively alters the athermal behavior. This is visible in Figure 3, where representative model calculations show the appearance of a minimum which shifts toward the critical density z_c^{HTA} as $t \to \Theta$.

In the protein limit ($R \ll R_g$), including thermal interactions within the RMPY/HTA closure leads to a shift of the attractive minimum located at z^* under athermal conditions toward z_c^{HTA}, i.e., toward higher polymer densities. This shift is accompanied by a simultaneous deepening of the minimum; at $t = \Theta$, eqs 18, 22, and 25 lead to the estimate that $B_2^{cc}/B_2^{HS} \sim -(R_g/R)(R_g/a)^{1/3}$ at $z = z_c^{HTA}$. Both of these trends, the deepening and simultaneous shift of the minimum from z^* toward z_c^{HTA} as t is reduced toward Θ, are seen in Figure 4 which shows model calculations relevant to the proteinlike limit.

Qualitatively similar effects, but of more pronounced magnitude, are found when the Flory−Huggins theory for t_s/Θ is used. Stronger thermal enhancement of the depletion effect is expected, given the systematically larger effects on ξ_ρ found within the Flory−Huggins theory. As t/Θ is lowered from its athermal value toward Θ, a minimum appears in B_2^{cc}/B_2^{HS} near z_c^{FH} in the colloid limit; for a given value of t/Θ, this minimum is deeper (more attractive) than that found based on the

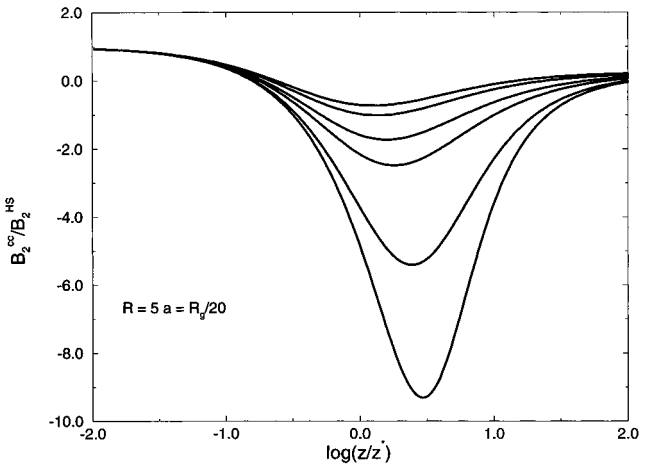

Figure 4. B_2^{cc}/B_2^{HS} as a function of log(z/z^*) under thermal conditions based on the RMPY/HTA closure in the $R \ll R_g$ protein limit. In all cases, $R = 5a$ and $R_g = 10^2a$; the curves correspond to $t/\Theta = \infty$, 5, 2, 1.5, 1.1, and 1.0 from top to bottom.

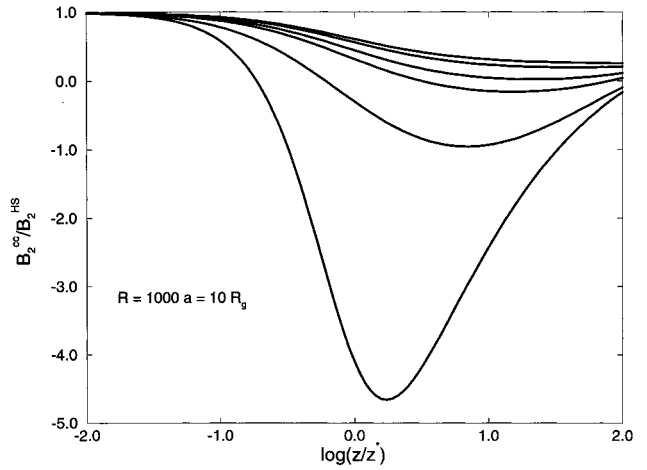

Figure 5. Same as Figure 3 but based on Flory−Huggins theory for ξ_ρ^{th}.

RMPY/HTA closure, and occurs at a lower polymer density as $z_c^{FH} \approx z^* < z_c^{HTA}$. Figure 5 shows results for B_2^{cc}/B_2^{HS} based on the Flory−Huggins theory of the polymer−solvent spinodal for the same values of R/R_g and t/Θ as were used in the RMPY/HTA-based calculations of Figure 3. In the protein limit, the minimum present at z^* under athermal conditions deepens as t/Θ is reduced; this increase in depth is now *not* accompanied by the shift to higher densities that was found for the RMPY/HTA treatment of the spinodal. At $t = \Theta$, eqs 18, 23, and 25 lead to the estimate that $B_2^{cc}/B_2^{HS} \sim -(R_g/R)\sqrt{N}$ near $z_c^{FH} \approx z^*$, indicating the stronger thermal effects found with use of the Flory−Huggins theory for the spinodal. The calculations shown in Figure 6, which use the same parameters employed in Figure 4, show the rapid deepening of the minimum at ϕ_c^{FH} relative to both the athermal result and the corresponding predictions based on the RMPY/HTA closure approximation.

The strong attractive modification of B_2^{cc} caused by thermal enhancment of ξ_ρ in the vicinity of the critical point becomes clearer from examining the loci of Boyle points at which $B_2^{cc} \equiv 0$ under thermal conditions. Equations 18 and 25 show that the condition $B_2^{cc} = 0$

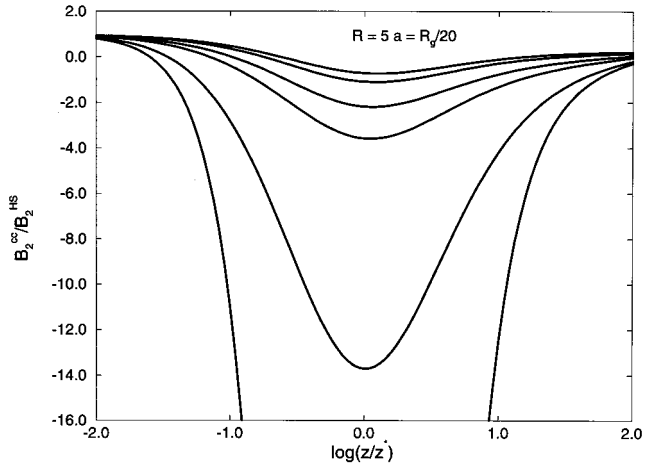

Figure 6. Same as Figure 4 but based on Flory−Huggins theory for ξ_ρ^{th}. The minimum value of $B_2^{cc}/B_2^{HS} \approx -165$ for $t = \Theta$.

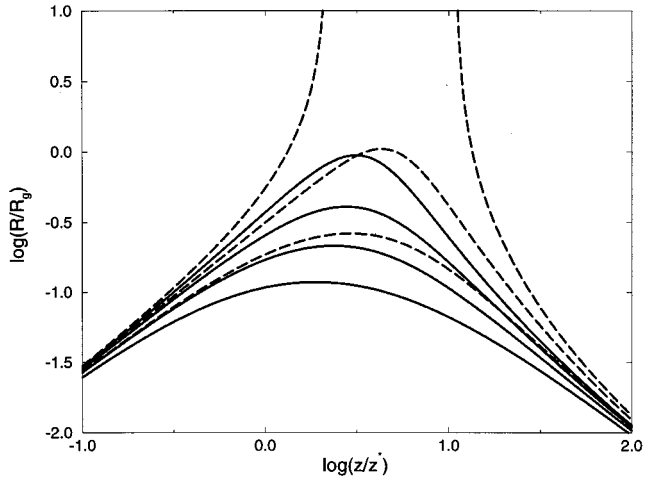

Figure 7. Values of log(R/R_g) for which $B_2^{cc} = 0$ shown as functions of log(z/z^*) within the RMPY/HTA theory for ξ_ρ^{th}. The solid and dashed lines correspond to $R_g = 10a$ and $R_g = 20a$, respectively. For each set of curves, $t/\Theta = \infty$, 2, 1.25, and 1.0 from bottom to top. The region *above* each curve corresponds to $B_2^{cc} > 0$.

can be expressed as

$$\frac{R}{R_g} = \left(\frac{\xi_\rho^{th}}{2R_g}\right)\left[\frac{8}{9x}\left(\frac{R_g}{\xi_\rho^{th}}\right) - 1\right]^{-1} \qquad (27)$$

where $x \equiv z/z^*$. Within the RMPY/HTA theory for t_s/Θ, eqs 5, 21, 25, and 27 give the values of R/R_g for which $B_2^{cc} \equiv 0$, as a function of R_g/a, z/z^*, and t/Θ. Numerical calculations of the loci of points satisfying eq 27 with the RMPY/HTA and Flory−Huggins theory predictions for ξ_ρ^{th} are shown in Figures 7 and 8, respectively. In all cases, the regions below and between the lines for each value of t/Θ and R_g/a (i.e., toward *smaller* values of R/R_g) correspond to domains where B_2^{cc} is negative/attractive. Within both the RMPY/HTA and Flory−Huggins theories for ξ_ρ^{th}, the domain of R/R_g and polymer concentrations over which B_2^{cc} is attractive increases dramatically as t/Θ is reduced. In the athermal case, B_2^{cc} is *always* positive/repulsive when $R > R_g$, and only in the "protein limit" when $R < R_g/(6\sqrt{2})$ do we find a pair of Boyle points corresponding to the minima in the curves

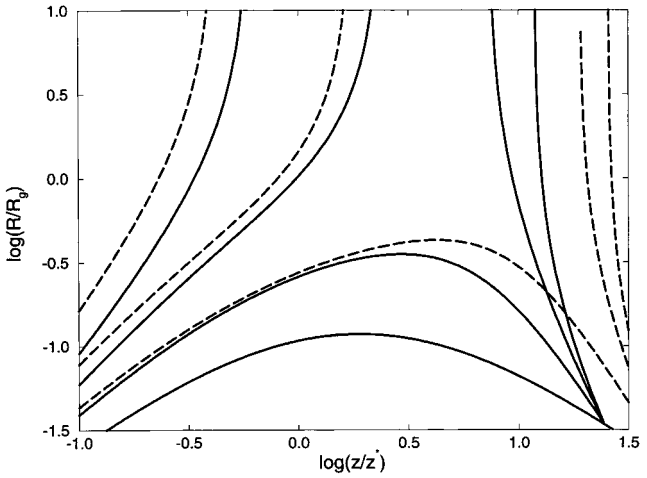

Figure 8. Same as Figure 7 but based on the Flory−Huggins theory for ξ_ρ^{th}.

for B_2^{cc} under athermal conditions shown in Figures 4 and 6. As t is reduced toward Θ, however, the attractive domain increases rapidly, and even for fairly modest chain lengths there appears a window of polymer concentrations around the critical density over which B_2^{cc} becomes attractive for *all* values of R/R_g, including the "colloid limit". Increasing the chain length N at *fixed* t/Θ enhances the attractive thermal modification of B_2^{cc}, as t_c approaches nearer Θ with increasing N in both the RMPY/HTA and Flory−Huggins theory, and the enhancement of ξ_ρ^{th} becomes more effective. The greater proximity of t_c to Θ for modest values of N predicted by the Flory−Huggins theory as compared to the RMPY/HTA calculation explains the notably larger enhancement of the attractive domain in Figure 8 relative to Figure 7 for equal values of t/Θ.

The preceding discussion has outlined the major qualitative effects of including thermal interactions within either the RMPY/HTA or Flory−Huggins theories on B_2^{cc}/B_2^{HS}. More quantitative estimates can be obtained from the criterion that the polymer−polymer thermal interactions are strong enough to induce either a 10% attractive modification in B_2^{cc}/B_2^{HS} relative to its athermal value or that the modification be strong enough to make B_2^{cc} negative at a given polymer concentration. The latter criterion is of limited utility in the "protein limit" where B_2^{cc} assumes negative values near z^* even under athermal conditions.

Equations 5, 18, and 25 show that the ratio B_2^{cc}/B_2^{HS} is a function of the variables R/R_g, z/z^*, and t/t_s alone. For concreteness, we focus attention on the dilute-semidilute crossover concentration z^*, and predictions based on the RMPY/HTA theory for ξ_ρ^{th}, which we believe are more accurate than their Flory−Huggins analogues. At this concentration, the ratio B_2^{cc}/B_2^{HS} is reduced by 10% relative to its athermal value at $t/t_s \approx$ 90, 6, and 4 for $R/R_g = 0.1$, 1, a value and in the "colloid limit" ($R \gg R_g$), respectively. In all cases, thermal polymer concentration fluctuations at the semidilute crossover point begin to influence the depletion attraction effect at a rather remarkably large distance from the spinodal temperature. B_2^{cc}/B_2^{HS} is most sensitive to thermal interactions in the "protein limit". This is physically reasonable, as under these conditions $\xi_\rho^{th} \gg R$ and modest fractional changes in ξ_ρ^{th} may still be significant on the particle size length scale R.

The condition that $B_2^{cc} = 0$ at $z = z^*$ is satisfied at $t/t_s \approx 1.2$ in the "colloid limit" ($R \gg R_g$), and at $t/t_s \approx 1.4$ when $R = R_g$. This again indicates that as R/R_g is increased at a given polymer concentration, closer approach to the spinodal envelope becomes necessary to achieve a similar degree of attractive thermal modification to B_2^{cc}/B_2^{HS}. The prediction that significant changes in B_2^{cc}/B_2^{HS} can be achieved for relatively large values of t/t_s may be of relevance in understanding experimental measurements of B_2^{cc} between globular protein molecules in polymer solutions at room temperature.[34] For example, the existence of an underlying UCST or LCST-type demixing transition as much as 100 K away from room temperature would correspond to $t/t_s \approx 1.3$ and could markedly alter theoretically predicted values of B_2^{cc}/B_2^{HS} in the attractive direction.

Finally, as the critical point is approached ($t \to t_c^+$), $B_2^{cc}/B_2^{HS} \to -\infty$ as $(R_g^2/\sigma R)\ (t_c/t - 1)^{-1}$. On the other hand, for $t > \Theta$ and polymer concentrations far removed from the semidilute crossover or critical value, that is $z \ll z^*$ or $z \gg z_{crit}$, thermal fluctuation effects are greatly reduced as seen in Figures 3−6.

C. Thermal Effects on $\beta\delta\mu_c$. The dimensionless particle insertion free energy, $\beta\delta\mu_c$, under thermal conditions is calculated from the compressibility route expression of eq 17 with the replacement $\xi_\rho \to \xi_\rho^{ath}/\sqrt{1-t_s/t}$ in eq 11 for $\hat{C}_{pc}(0)$. Since, for a fixed reduced temperature t, the ratio t_s/t is a function of reduced polymer density z, the integration in eq 17 must in general be performed numerically. General qualitative features may, however, be understood in analytic terms. As for the earlier discussion of B_2^{cc}, for simplicity we focus attention on $t = \Theta$.

Within the RMPY/HTA closure, in the colloid limit the inequality $\xi_\rho^{th} \le R_g/\sqrt{2} \ll R$ holds for all polymer densities at $t = \Theta$. Equations 7 and 8 for the compressibility route polymer osmotic pressure, together with eqs 11 and 17, show that, under these conditions

$$\beta\delta\mu_c \approx \beta P_{th} V_{sphere} \tag{28}$$

where P_{th} is the compressibility route polymer osmotic pressure under thermal conditions. The reduction in pressure from P_{ath} to P_{th} under thermal conditions thus leads to a smaller value for the particle insertion free energy and hence enhanced solubility. As discussed in earlier work employing the RMPY/HTA closure, at $t = \Theta$ *both* the second *and* third polymer−polymer virial coefficients vanish in the long-chain limit;[19] the simultaneous vanishing of the third virial coefficient was related to neglect of *explicit* three body (solvent-mediated) interactions between polymer segments in the present theory. This feature, combined with the previous discussion of ξ_ρ^{th}, shows that, at $t = \Theta$, linear behavior of $\beta\delta\mu_c \sim (R^3\ \rho_p/N)$ is followed for $z \le z_c^{HTA} \sim N^{-1/3}$. Above the critical density, $\xi_\rho^{th}/\sigma \sim z^{-3/2}$ at $t = \Theta$, implying that the pressure grows such as $\beta P_{th}\sigma^3 \sim z^4$; the athermal scaling behavior ($\beta P_{ath}\sigma^3 \sim z^3$) is altered by the vanishing in the large N limit of the third polymer−polymer virial coefficient in this theory at $t = \Theta$. Thus, for $z > z_c^{HTA}$, $\beta\delta\mu_c \sim (a/\sigma)(R/\sigma)^3 z^4$; the athermal behavior ($\beta\delta\mu_c \sim (R/\sigma)^3 z^3$) is recovered when $z > \sigma/a$, i.e., when $\xi_\rho^{ath} \approx a$.

The range of polymer densities over which $\beta\delta\mu_c$ increases linearly with z in the $R \ll R_g$ protein limit

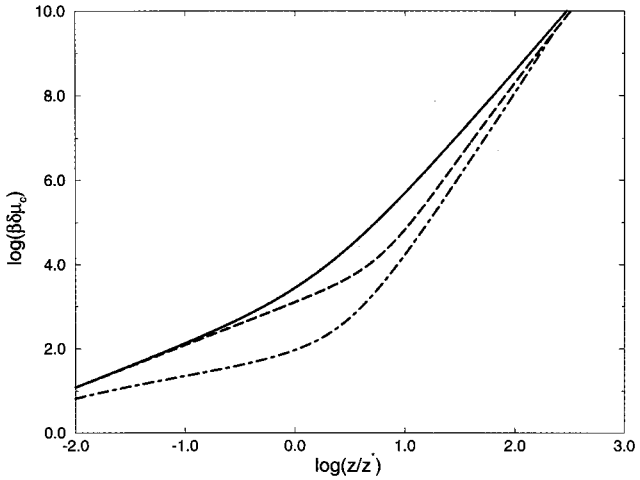

Figure 9. Logarithm of the dimensionless free energy of sphere insertion as a function of $\log(z/z^*)$ under thermal conditions for the colloid limit. The solid line shows the $t \to \infty$ athermal result, and the dashed and dot−dashed lines show predictions at $t = \Theta$ from the RMPY/HTA and Flory−Huggins theories for ξ_ρ^{th}, respectively. The RMPY/HTA based calculation uses $R = 10^3 a$ and $R_g = 10^2 a$, while the Flory−Huggins based result employs $R = 10^3\sigma$ and $R_g = 10^2\sigma$.

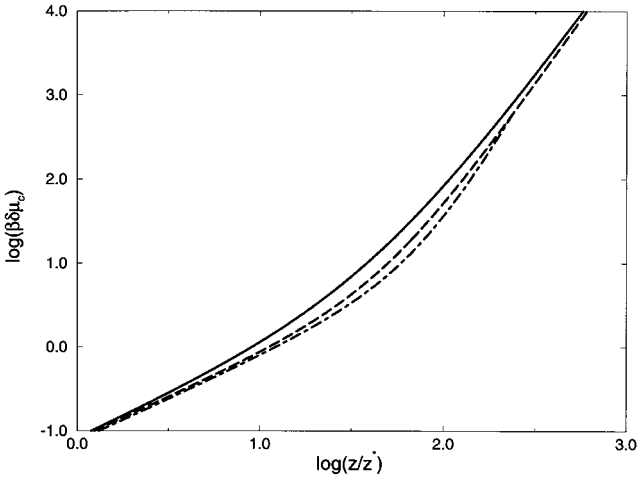

Figure 10. Same as Figure 9 but in the protein limit. The RMPY/HTA theory calculations uses $R = 5a$ and $R_g = 10^2 a$, while the calculation based on Flory−Huggins theory employs $R = 5\sigma$ and $R_g = 10^2\sigma$.

again extends up to the point at which the particle size and mesh length are roughly equal, $\xi_\rho^{th} \approx R$. The corresponding density, denoted $z^\dagger$, is $z^\dagger \approx (\sigma/R)^{2/3}\delta^{-1/3}$ at $t = \Theta$, and is higher than both z_c^{HTA} and also the value of $z^\dagger$ under athermal conditions. For densities $z < z^\dagger$, $\beta\delta\mu_c \sim (R/\sigma)z$. Above $z^\dagger$, $\xi_\rho^{th} < R$, and quartic behavior $\beta\delta\mu_c \sim (a/\sigma)(R/\sigma)^3 z^4$ is predicted, as was found for the colloid limit above z_c^{HTA}. Given the modest values of R appropriate to the protein limit ($R \approx 3-5\sigma$), the separation between $z^\dagger$ and $z \approx 1/\delta$ may not be large enough to permit clear establishment of the quartic dependence of $\beta\delta\mu_c$ in the protein limit.

Similar behavior is seen in both the colloid and protein limits when the Flory−Huggins result for t_s/Θ is used to estimate ξ_ρ^{th}. In the colloid limit, regimes with approximately linear and quartic dependences of $\beta\delta\mu_c$ on z are separated by the density at which the behavior $\xi_\rho^{th} \sim z^{-3/2}$ sets in the Flory−Huggins theory; as indicated previously, this regime is established in the neighborhood of $z_1 \sim N^{-1/3}$. The polymer-density dependences of $\beta\delta\mu_c$ predicted by the Flory−Huggins and RMPY/HTA theories of the spinodal are therefore very similar; however, at sufficiently low densities, $z < z^* \approx z_c^{FH}$, the increase in ξ_ρ^{th} above ξ_c in the Flory−Huggins theory gives rise to a slightly weaker, sublinear growth of $\beta\delta\mu_c$ with z . The analogous extension of the linear domain over which $\beta\delta\mu_c \sim (R/\sigma)z$ is found in the protein limit as well, and, as for the RMPY/HTA theory, terminates when $\xi_\rho^{th} \approx R$; for the modest values of R relevant to this case, the subsequent quartic regime may not be clearly visible.

Model calculations of $\beta\delta\mu_c$ for parameters relevant to the colloid and protein limits are shown for both the Flory−Huggins and RMPY/HTA theories of the spinodal boundary in Figures 9 and 10. As the temperature dependence of $\beta\delta\mu_c$ is relatively weak, we have for clarity displayed only results obtained at $t = \Theta$ and in the athermal limit. In both the colloid and protein limits, the thermal suppression is stronger in the Flory−Huggins than in the RMPY/HTA-based calculations. This is due to the stronger enhancement of ξ_ρ and closer proximity of t_c to Θ in the former theory. Note the crossover from linear to approximately quartic dependence of $\beta\delta\mu_c$ on z at near the critical density z_c^{HTA} or ϕ_c^{FH} in the colloid limit (Figure 9); the crossover appears more rounded and broader in the Flory−Huggins based results due to the broad peak in ξ_ρ^{th} (Figure 2) in the vicinity of the critical density. The difference between the Flory−Huggins and RMPY/HTA based calculations at $t = \Theta$ are smaller in the protein limit (Figure 10), and the quartic regime $\beta\delta\mu_c \sim z^4$ is not clearly established in either case due to the small range of densities satisfying $\xi_\rho^{ath} > a$ and $\xi_\rho^{th} < R$; the inclusion of thermal polymer−polymer segmental interactions thus has a relatively minor effect on $\beta\delta\mu_c$ calculated from the compressibility route for the proteinlike limit.

IV. Discussion

The present work has generalized our previous analytic theory[1] for dilute suspensions of hard spheres in athermal polymer solutions to include thermal interactions between the polymer segments and variable solvent quality. Methods for including polymer−colloid and colloid−colloid thermal interaction potentials are discussed in the Appendix. Results have been presented for the temperature and polymer concentration dependences of the density screening length, colloid−colloid second virial coefficient, and free energy for sphere insertion into a polymer solution.

Incorporating polymer−polymer segmental attractive interactions significantly enhances the range of the polymer-induced attractive depletion potential in the vicinity of the polymer−solvent critical demixing transition. This is not a surprising result, and occurs due to the long-ranged critical fluctuations in the polymer density, a mechanism independent of the specific theory (Flory−Huggins or RMPY/HTA) used to describe the underlying polymer−solvent phase transition. The details of the behavior of B_2^{cc} and of ξ_ρ^{th} are, however, sensitive to the theory employed for the phase transition, as ξ_ρ^{th} depends strongly on distance from the spinodal line. Thus, for a fixed value of t/Θ, the Flory−Huggins theory predicts a stronger thermal enhance-

ment of the polymer-induced attraction than does the RMPY/HTA theory. However, the latter theory is in much better agreement with experimental measurements of critical polymer concentrations and the thermal density screening length of polymer solutions.[16,33]

Our results are relevant to situations in which depletion-induced flocculation, or polymer−particle phase separation, is thought to occur at near-Θ conditions.[35] Within PRISM-PY theory, proximity to the critical point is capable of creating an attractive minimum in B_2^{cc} near the critical polymer density which is entirely absent from the corresponding athermal situation in the $R \gg R_g$ colloid limit or $R \approx R_g$ "crossover" cases. Coupling to long-wavelength critical fluctuations appears to have significant consequences even remarkably far removed from t_c if the polymer concentration is in the semidilute crossover or critical composition range. The enhancement of the depletion attraction by such a mechanism is *not* specific to the macromolecular nature of the depletant but could conceivably operate even for small molecule depletants sufficiently near a critical point, although the details would be nonuniversal. Of course, the fact that the "bare" (athermal) density screening length can be very large for macromolecules greatly enhances their ability to mediate "long range" depletion attractions between spherical particles. It is this feature which leads to the enhanced sensitivity of small particles ($R \leq R_g$) to thermal polymer concentration fluctuations compared to large colloidal spheres.

In related work,[14] we have shown that inclusion of packing diameter nonadditivity athermal effects can also enhance the attractive depletion effect by increasing the *strength* though *not* the *range* of the polymer-mediated interaction between particles. The coupling to critical fluctuations is a physically very different mechanism, as it operates by increasing the *range* and *not* the *strength* (as judged by $g_{cc}(d_{cc})$) of the depletion potential.

Under near-Θ conditions, the minimum in B_2^{cc} becomes deeper (more attractive) as the polymer molecular weight is increased; also, at polymer densities above the critical point, B_2^{cc} again increases to a positive (repulsive) value. The latter trend may relate to the controversial phenomenon of polymer-induced restabilization[36] reported by some workers at polymer concentrations above the semidilute crossover ϕ^*. One must be cautious about such an interpretation, however, as it has been suggested that the restabilization phenomenon may involve kinetic effects due to barriers which appear in the potential of mean force at high polymer packing fractions[6] ($\rho_p > \rho^{**}_p$). Such barriers arise naturally in PRISM calculations for concentrated (but *not* semidilute) solutions which do full justice to the nonzero chain thickness and include high polymer density packing effects.[37] The latter are absent from the present analytic theory applicable under dilute and semidilute conditions, which represents the polymer molecule as a Gaussian thread.

It would be of great interest to test key features of the present theory through suitably designed experimental and computer simulation studies. Experimental studies on polymer solutions with chains of a fixed molecular weight could be performed over a range of temperatures approaching the polymer−solvent demixing point. Absence of charges from both the polymer and the spheres and refractive-index matching to eliminate thermal dispersion interactions could ensure that the primary thermal interactions present are those between the polymer segments themselves. An unambiguous representation of the sphere−sphere and sphere−polymer segmental interactions as being of the purely hard core excluded volume type may be more directly achieveable in computer simulations, in which it would be crucial to include the excluded volume interactions between *all* pairs of components. Simulations for particles of modest size ($R \leq R_g$) should be the most tractable case.

In future work, we shall present results of numerical PRISM studies on finite thickness semiflexible chains with solute spheres of different diameters under athermal conditions. Preliminary results of such calculations are consistent with our analytic theoretical predictions. Generalization of the PRISM−PY theory of polymer−particle mixtures to treat the finite particle concentration case is discussed elsewhere by Fuchs and Schweizer.[38]

Acknowledgment. We thank Dr. M. Fuchs for many helpful discussions. This work was supported by the Division of Materials Science, Office of Basic Energy Sciences, U.S. Department of Energy, in cooperation with Oak Ridge National Laboratory, and the UIUC Frederick Seitz Materials Research Laboratory, Grant No. DEFG02-96ER45439.

Appendix

Here we present general results for the inclusion of thermal contributions to the polymer-colloid and colloid−colloid interactions within the site−site mean spherical approximation (MSA). The MSA closure allows analytic solutions to be obtained for the correlation functions, and has been employed by previous workers for the case of binary mixtures of hard spheres interacting via Yukawa potentials.[39] The MSA applied to a system interacting via a potential which can be decomposed into a hard core and an attractive tail prescribes the value of the direct correlation function outside the core:[39]

$$C_{MM'}(r) = -\beta v_{MM'}(r), \quad r > d_{MM'} \tag{29}$$

Here $v_{MM'}(r)$ is the nonhard core, or "tail", component of the potential. In what follows, we assume that the thermal contribution to the polymer−colloid interaction is of the Yukawa form:

$$v_{pc}(r) = \epsilon_{pc}\left(\frac{a}{r}\right)e^{-r/a} \tag{30}$$

The polymer−colloid direct correlation function under thermal conditions is chosen to satisfy eqs 3, 9, and 29, and the strength of the Dirac delta function contribution at the sphere surface is chosen to enforce the boundary condition that $g_{pc}(r \to R+) = 0$. It may be verified that the following correlation functions satisfy these requirements:

$$C_{pc}(r) = C_{pc}^{(1)}(r) + C_{pc}^{(2)}(r)$$

$$C_{pc}^{(1)}(r) = -\frac{1}{12}\left(\frac{\sigma}{\xi_\rho}\right)^2, \quad r < R$$

$$= -\frac{1}{t}\left(\frac{R}{r}\right)e^{-(r-R)/a}, \quad r > R$$

$$C_{pc}^{(2)}(r) = \left[\frac{1}{t\left(\frac{1}{\xi_\rho}+\frac{1}{a}\right)} - \frac{\sigma^2}{12}\left(\frac{1}{R}+\frac{1}{\xi_\rho}\right)\right]\delta(r-R),$$

$$h_{pc}(r) = -1, \quad r < R,$$

$$= -\left(\frac{R}{r}\right)e^{-(r-R)/\xi_\rho} - \frac{12}{\sigma^2 t}\left(\frac{R}{r}\right)\frac{1}{\left(\frac{1}{a^2}-\frac{1}{\xi_\rho^2}\right)}[e^{-(r-R)/\xi_\rho} - e^{-(r-R)/a}], \quad r > R \quad (31)$$

Here

$$t \equiv \frac{k_B T}{\epsilon_{pc}}\left(\frac{R}{a}\right)e^{R/a} \quad (32)$$

Equations 31 and 32 are now used to obtain the polymer-induced contributions to the colloid−colloid correlation functions, determined by the function $W(r)$ of eq 12. Equations 12, 31, and 32, plus tedious but straightforward analysis, lead to the following expression for $W(r)$:

$$W(r) = -\frac{\pi r z}{12\sigma} + \frac{\pi R z}{3\sigma} + \frac{4a^2\pi R z}{\sigma^3 t} - \frac{4a^3\pi R z}{r\sigma^3 t} - \frac{2a\pi r R z}{\sigma^3 t} + \frac{4a\pi R^2 z}{\sigma^3 t} - \frac{4a^2\pi R^2 z}{r\sigma^3 t} + \frac{\pi r^3 z}{144\sigma\xi_\rho^2} - \frac{\pi r R^2 z}{12\sigma\xi_\rho^2} + \frac{\pi R^3 z}{9\sigma\xi_\rho^2} - \frac{\pi r R z}{6\sigma\xi_\rho} + \frac{\pi R^2 z}{3\sigma\xi_\rho} + \frac{4a\pi R^2\xi_\rho z}{r\sigma^3 t} + \frac{24a^2\pi R^2\xi_\rho^2 z}{r\sigma^5 t^2} + \frac{4\pi e^{-r/a}}{(a+\xi_\rho)^2}\left[\frac{a^5 R z}{r\sigma^3 t} + \frac{a^4 R^2 z}{r\sigma^3 t} + \frac{2a^4 R\xi_\rho z}{r\sigma^3 t} + \frac{a^3 R^2\xi_\rho z}{r\sigma^3 t} - \frac{6a^4 R^2\xi_\rho^2 z}{r\sigma^5 t^2} + \frac{a^3 R\xi_\rho^2 z}{r\sigma^3 t}\right] + \frac{24a^2\pi R^2\xi_\rho^4 z}{r\sigma^5 t^2(a+\xi_\rho)^2} + \frac{2a\pi r R\xi_\rho z}{\sigma^3 t(a+\xi_\rho)} - \frac{4a\pi R^2\xi_\rho z}{\sigma^3 t(a+\xi_\rho)} - \frac{48a^2\pi R^2\xi_\rho^3 z}{r\sigma^5 t^2(a+\xi_\rho)}, \quad r < 2R$$

$$W(r) = \pi R z[12a^7 e^{-r/a}\sigma^2 t(1-e^{2R/a}) + 12a^6 R\sigma^2 t e^{-r/a}(1+e^{2R/a}) + a^4 R\sigma^4 t^2 e^{-(r-2R)/\xi_\rho} + 12a^5 R\sigma^2 t\xi_\rho e^{-r/a}(e^{2R/a}-1) + 72a^6 R\xi_\rho^2 e^{-r/a}(e^{2R/a}-1) + 72a^5 r R\xi_\rho^2 e^{-(r-2R)/a} - 144a^5 R^2\xi_\rho^2 e^{-(r-2R)/a} + 24a^5\sigma^2 t\xi_\rho^2 e^{-r/a}(e^{2R/a}-1) - 12a^4 e^{-(r-2R)/a} R\sigma^2 t\xi_\rho^2 - 24a^4 e^{-(r-2R)/\xi_\rho} R\sigma^2 t\xi_\rho^2 - 12a^4 e^{-r/a} R\sigma^2 t\xi_\rho^2 - 2a^2 e^{-(r-2R)/\xi_\rho} R\sigma^4 t^2\xi_\rho^2 - 144a^5 R\xi_\rho^3 e^{-r/a}(e^{2R/a}-1) - 12a^3 R\sigma^2 t\xi_\rho^3 e^{-r/a}(e^{2R/a}-1) - 72a^4 e^{-(r-2R)/a} R\xi_\rho^4 + 144a^4 e^{-(r-2R)/\xi_\rho} R\xi_\rho^4 - 72a^4 e^{-r/a} R\xi_\rho^4 - 72a^3 e^{-(r-2R)/a} r R\xi_\rho^4 + 144a^3 e^{-(r-2R)/a} R^2\xi_\rho^4 - 12a^3 e^{-r/a}\sigma^2 t\xi_\rho^4(e^{2R/a}-1) + 24a^2 e^{-(r-2R)/\xi_\rho} R\sigma^2 t\xi_\rho^4 + e^{-(r-2R)/\xi_\rho} R\sigma^4 t^2\xi_\rho^4]/(3r\sigma^5 t^2(\xi_\rho - a)^2(\xi_\rho + a)^2), \quad r > 2R \quad (33)$$

Equation 33 for $W(r)$ reduces to eq 13 when $t \to \infty$, i.e., when the polymer−colloid interaction reverts to being purely athermal. The correlation functions $g_{cc}(r)$ and $C_{cc}(r)$ may now be obtained from eqs 14 and 33.

If there is an additional colloid−colloid thermal interaction, $v_{cc}(r)$, the appropriate $g_{cc}(r)$ and $C_{cc}(r)$ values within the MSA closure follow immediately from eqs 14, 29, and 33. The function $W(r)$, which describes the polymer-mediated interaction, is *not* affected by the thermal colloid−colloid interaction and is still given by eq 33; this decoupling is valid only when the colloidal species is at infinite dilution, and will not apply at finite concentrations of the spheres. Within the MSA closure, $g_{cc}(r)$ and $C_{cc}(r)$ are then given by

$$g_{cc} = 0, \quad r < d_{cc}$$

$$= 1 - \beta v_{cc}(r) + W(r), \quad r > d_{cc}$$

$$C_{cc}(r) = -(1 + W(r)), \quad r < d_{cc}$$

$$= -\beta v_{cc}(r), \quad r > d_{cc} \quad (34)$$

Note that $W(r)$ in eq 33 does *not* change even if we consider the nonadditive diameter problem[14] ($d_{cc} \neq 2R$); thus the results of eqs 33 and 34 may be used to consider cases involving *both* thermal interactions as well as nonadditivity in the hard core diameters. This simplification, which allows a unified solution to the general thermal nonadditive diameter problem, is peculiar to the infinite dilution limit and does not hold at finite colloid concentrations.

References and Notes

(1) Chatterjee, A. P.; Schweizer, K. S. *J. Chem. Phys.* **1998**, *109*, 10464, 10477.
(2) Asakura, S.; Oosawa, F. *J. Chem. Phys.* **1954**, *22*, 1255; *J. Polym. Sci.* **1958**, *33*, 183.
(3) Gast, A. P.; Hall, C. K.; Russell, W. B. *J. Colloid Interface Sci.* **1983**, *96*, 251; **1986**, *109*, 161.
(4) Vincent, B.; Edwards, J.; Emmett, S.; Jones, A. *Colloids Surf.* **1986**, *18*, 261.
(5) Lekkerkerker, H. N. W.; Poon, W. C. K.; Pusey, P. N.; Stroobants, A.; Warren, P. B. *Europhys. Lett.* **1992**, *20*, 559. Lekkerkerker, H. N. W.; Stroobants, A. *Physica A* **1993**, *195*, 387.
(6) Sharma, A.; Tan, S. N.; Walz, J. Y. *J. Colloid Interface Sci.* **1997**, *190*, 392; **1997**, *191*, 236.
(7) Mao, Y.; Cates, M. E.; Lekkerkerker, H. N. W. *Phys. Rev. Lett.* **1995**, *75*, 4548.
(8) Joanny, J. F.; Leibler, L.; de Gennes, P. G. *J. Polym. Sci., Polym. Phys. Ed.* **1979**, *17*, 1073.
(9) Eisenriegler, E.; Hanke, A.; Dieterich, S. *Phys. Rev. E* **1996**, *54*, 1134.
(10) Meijer, E. J.; Frenkel, D. *J. Chem. Phys.* **1994**, *100*, 6873.
(11) Dickman, R.; Yethiraj, A. *J. Chem. Phys.* **1994**, *100*, 4683.
(12) Vincent, B.; Luckham, P. F.; Waite, F. A. *J. Colloid Interface Sci.* **1979**, *73*, 508.
(13) Milling, A.; Vincent, B.; Emmett, S.; Jones, A. *Colloids Surf.* **1991**, *57*, 185.
(14) Chatterjee, A. P.; Schweizer, K. S. To be submitted for publication in *J. Colloid Interface Sci.*
(15) de Gennes, P. G. *Scaling Concepts in Polymer Physics*; Cornell University Press: Ithaca, NY, 1979.
(16) Chatterjee, A. P.; Schweizer, K. S. *J. Chem. Phys.* **1998**, *108*, 3813.
(17) Chandler, D.; in *Studies in Statistical Mechanics VIII*; Montroll, E., Lebowitz, J. L., Eds.; North-Holland: Amsterdam, 1982. Chandler, D.; Andersen, H. C. *J. Chem. Phys.* **1972**, *57*, 1930.
(18) Schweizer, K. S.; Curro, J. G. *Adv. Polym. Sci.* **1994**, *116*, 319; *Adv. Chem. Phys.* **1997**, *98*, 1.
(19) Chatterjee, A. P.; Schweizer, K. S. *Macromolecules* **1998**, *31*, 2353.

(20) Grayce, C. J.; Schweizer, K. S. *J. Chem. Phys.* **1994**, *100*, 6846. Grayce, C. J.; Yethiraj, A.; Schweizer, K. S. *J. Chem. Phys.* **1994**, *100*, 6857. Melenkevitz, J.; Curro, J. G.; Schweizer, K. S. *J. Chem. Phys.* **1993**, *99*, 5571.
(21) Yethiraj, A. *Phys. Rev. Lett.* **1997**, *78*, 3789.
(22) Kirkwood, J. G.; Buff, F. P. *J. Chem. Phys.* **1951**, *19*, 774.
(23) Hill, T. L. *Statistical Mechanics: Principles and Selected Applications*; McGraw-Hill: New York, 1956.
(24) Saeki, S.; Kuwahara, N.; Nakata, M.; Kaneko, M. *Polymer* **1976**, *17*, 685.
(25) Schweizer, K. S.; Yethiraj, A. *J. Chem. Phys.* **1993**, *98*, 9053.
(26) Schweizer, K. S. *Macromolecules* **1993**, *26*, 6050.
(27) Guenza, M.; Schweizer, K. S. *Macromolecules* **1997**, *30*, 4205.
(28) Flory, P. J. *Principles of Polymer Chemistry*; Cornell University Press: Ithaca, NY, 1953.
(29) Perzynski, R.; Delsanti, M.; Adam, M. *J. Phys. (Fr.)* **1987**, *48*, 115. Xia, K. Q.; An, X. Q.; Shen, W. G. *J. Chem. Phys.* **1996**, *105*, 6018.
(30) Panagiotopoulos, A. Z.; Wong, V.; Floriano, M. A. *Macromolecules* **1998**, *31*, 912.
(31) Chatterjee, A. P.; Schweizer, K. S. Unpublished material.
(32) Melnichenko, Y. B.; Wignall, G. D. *Phys. Rev. Lett.* **1997**, *78*, 686.
(33) Kinugasa, S.; Hayashi, H.; Hamada, F.; Nakajima, A. *Macromolecules* **1986**, *19*, 2832.
(34) Kulkarni, A. M.; Chatterjee, A. P.; Schweizer, K. S.; Zukoski, C. F., submitted for publication in *Langmuir*.
(35) Poon, W. C. K.; Selfe, J. S.; Robertson, M. B.; Ilett, S. M.; Pirie, A. D.; Pusey, P. N. *J. Phys. II* **1993**, *3*, 1075.
(36) Ye, X.; Narayanan, T.; Tong, P.; Huang, J. S. *Phys. Rev. Lett.* **1996**, *76*, 4640.
(37) Yethiraj, A.; Hall, C. K.; Dickman, R. *J. Colloid Interface Sci.* **1992**, *151*, 102.
(38) Fuchs, M.; Schweizer, K. S. To be submitted for publication.
(39) Hansen, J. P.; McDonald, I. R. *Theory of Simple Liquids*; Academic Press: New York, 1986.

MA981473H